Pressure Induced Reactivity of Solid CO by FTIR Studies

Matteo Ceppatelli,[†,‡] Anton Serdyukov,[§] Roberto Bini,*[,†,‡] and Hans J. Jodl[†,§]

LENS, European Laboratory for Nonlinear Spectroscopy, Via N. Carrara 1, I-50019 Sesto Fiorentino, Firenze, Italy, Dipartimento di Chimica dell'Università di Firenze, Via della Lastruccia 3, I-50019 Sesto Fiorentino, Firenze, Italy, and Fachbereich Physik, University of Kaiserslautern, Kaiserslautern, Germany

Received: January 20, 2009; Revised Manuscript Received: March 12, 2009

The pressure induced reactivity of carbon monoxide was investigated in a wide temperature range (100−400 K) completely avoiding any irradiation of the sample with visible or higher frequency light. FTIR spectroscopy was employed to monitor the reaction and infrared sensors for measuring the pressure. With this approach we have been able to separate the effects of the three variables (P, T and hν) that establish the conditions for the occurrence of the chemical reaction. A new instability boundary, not affected by the photoactivation of the reaction, is provided. The reaction has been studied in three different crystal phases (ϵ, δ, and β), but the small differences in the reaction products are ascribable to the temperature changes rather than to the crystalline arrangement. For $T < 300$ K the analysis of the IR spectra reveals the formation of an extended amorphous material formed, according to the vibrational assignment and to the kinetic data, by polycarbonyl linear chains containing a large amount of anhydride groups. For $T \geq 300$ K the formation of carbon dioxide and epoxy rings, and the simultaneous decrease of carbonyl species, let suppose a decarboxylation of the extended solid product. Once exposed to the atmosphere, the reaction product readily and irreversibly reacts with water giving rise to carboxylic groups.

1. Introduction

Chemical reactions can be induced in the simplest molecular systems by the application of suitable high pressure conditions.[1] The interest for these studies spans across several research fields: from the synthesis of novel materials having great technological interest, such as polymers[2,3] and ultrahard or high Tc superconductors,[4] to the knowledge of processes occurring in the Earth's interior or in astronomic objects.[5] The formation of extended covalently bonded solids at high pressure has been reported for two model molecules like CO_2[6,7] and N_2.[8,9] Both transformations require quite drastic pressure and temperature conditions, and the products cannot be recovered at ambient conditions. An irreversible transformation to an extended amorphous material has been on the contrary reported for carbon monoxide[10−15] with remarkable differences with respect to N_2. Despite the two molecules being isoelectronic and isostructural and the low pressure phase diagrams and crystal structures exhibiting striking similarities,[12] the instability threshold is 1 order of magnitude lower than in N_2 and it is strongly affected by laser irradiation.

The high pressure instability of CO at room temperature and 4.2 GPa under mild laser irradiation conditions (pressure calibration by the ruby fluorescence method) was first reported by Cromer et al. in a single crystal X-ray diffraction study.[16] Since this study, the reactivity of CO under pressure was reported several times in Raman and X-ray experiments.[10−12] In these studies the transformation threshold was shown to be temperature sensitive, changing from 12 GPa at 15 K to 4.6 GPa at 80 K and to 4.2 GPa at 300 K, but the effects of pressure and laser or X-ray irradiation were never separated. The reaction product showed a variable coloration from yellow to black depending on the history and on the irradiation conditions and two different products were suggested: poly(carbon suboxide) $(C_3O_2)_n$ and dimeric oxalic anhydride $(C_2O_3)_2$.[11] Experiments performed by irradiating compressed CO with several watts of green and blue laser lines revealed the formation of a heterogeneous product composed by CO_2 and by a solid product identified as a polymeric network containing vinyl ester repeating units.[13] The observation of CO_2 suggests that the mechanisms of the purely pressure induced and photoassisted reactions can be different. A very interesting insight on the microscopic reaction mechanism and on the product was provided by an ab initio molecular dynamics simulation study, in which a two-step reaction mechanism was proposed.[17] The first step consists of the formation of small polycarbonyl units (i.e., single bonds are formed between C atoms of different CO molecules), and it is followed by the opening of some C═O bonds, giving rise to 5-fold cycles each containing a C−O−C bridge and two carbonyl groups. These rings are interconnected through a network of polycarbonyl chains. No evidence of C−O bond breaking, of the formation of CO_2, and of any other of the products proposed in the earlier studies was found. More recently, a detailed study of the reactivity of CO under pressure was performed by using both the DAC and a large volume press to increase the amount of the reaction product (p-CO) for extended analytical investigations.[14,15] Differences in the reaction products synthesized in the "dark" (without photon irradiation), photoassisted, and high temperature (laser heated) reactions were reported and discussed. The recovered materials from all these reactions look pretty much the same: a polymeric network without long-range order, extremely photosensitive, metastable at ambient conditions where it decomposes by releasing CO_2 and CO, and readily reacting with atmospheric water. This material is also reported to be an interesting energetic material exploding under moderate NIR irradiation.[14] The core of this material was suggested to be formed by β-lactone rings and

* Corresponding author. E-mail: bini@chim.unifi.it.
† European Laboratory for Nonlinear Spectroscopy.
‡ Università di Firenze.
§ University of Kaiserslautern.

10.1021/jp900586a CCC: $40.75
Published on Web 04/15/2009

conjugated C═C bonds in a sort of highly perturbed polymeric carbon suboxide originated by the formation of CO_2 due to disproportion of the polymer.

From all these studies emerges the lack of a systematic analysis of the reaction in which the three parameters that set the reactive pathway and the kinetics (pressure, temperature and laser irradiation) are controlled. As a matter of fact, all the experiments reported in the literature somehow involve laser irradiation of the sample. Even in the so-called "dark" reaction reported in ref 15 the sample was irradiated to measure the Raman spectra. Only the separation of the different contributions allows the definition of the stability diagram not affected by photoinduced reactive processes. Also the characterization of the products and of the corresponding formation kinetics in different thermodynamic reaction conditions is mandatory for the identification of competitive processes.

In this study we have used FTIR spectroscopy to probe the phase diagram of CO along several isotherms in a wide range of temperature (100−400 K) to identify the stability boundary. The effects of laser irradiation and pressure were completely uncoupled by using IR sensors for pressure calibration allowing the obtainment of a new stability line. The kinetics of the pressure induced reaction was determined at all the investigated temperatures by monitoring high quality IR spectra as a function of time at constant pressure and temperature. The detailed spectroscopic analysis of the products by using FTIR spectroscopy along with the results of the kinetic studies provides a deep insight in the reaction dynamics.

2. Experimental Section

To separate the effects of pressure and laser irradiation, the ruby fluorescence method could not be used to determine the local pressure of the sample inside the DAC. In all the experiments we have employed the pressure shift of the antisymmetric stretching mode of the NO_2^- ion that presents, at ambient pressure, a narrow intense IR absorption band at 1278.7 cm^{-1}. In this method, carefully described elsewhere,[18] a freshly recrystallized solid solution of $NaNO_2$ in NaBr (∼1% in weight) is first finely mashed and successively dried for 12 h at 100 °C. The powder is then inserted in the rhenium gasket (∼150 μm in diameter and ∼50 μm thick) and compressed between the diamonds to obtain a transparent pellet. IR spectra are employed to check the presence of water or other impurities. The pellet is then scratched to reduce its thickness. By monitoring the IR spectra and comparing them to the spectrum of the initial pellet of known thickness, we reduced the thickness of the salt mixture to the desired value (∼10 μm). By this method we have been able to produce very thin CO samples, thus reducing the product IR absorption bands for a careful study of the time evolution of the reaction. Once the salt substrate was prepared, the membrane DAC was placed in a stainless steel vessel for the cryogenic loading of CO. The vessel was pumped several hours to $\sim 10^{-3}$ bar and then cooled by using liquid nitrogen. CO from Rivoira (≥99.99%) was liquified in the vessel to fill the sample chamber. Pressure was applied in the membrane to seal the sample and the cell was then warmed to room temperature. Initial pressures never exceeded 2 GPa. IR spectra were measured by a FTIR spectrometer (Bruker IFS 120 HR) suitably modified to allow high pressure measurements.[19] The instrumental resolution was better than 1 cm^{-1}. Low temperature measurements were performed by coupling to the spectrometer a closed-cycle cryostat, whereas for the measurement above room temperature we employed a resistive heating of the cell. In the two kinds of experiments the temperature was measured close to the diamond by a Si-diode and a thermocouple, respectively. Because the NO_2^- sensors were tested only at room temperature[18] we performed new calibration experiments by measuring the IR spectra of the salt as a function of pressure at 100, 200, 350, and 400 K determining the local pressure by the ruby fluorescence technique. These data are reported in Figure 1. As can be seen, the pressure shift of the antisymmetric stretching mode of NO_2^- ($\Delta\nu$) is quite insensitive to the temperature variation up to about 5 GPa, but above this pressure the room temperature calibration cannot be used for the 100 and 200 K experiments. A fit function of the type

$$P = a_1\Delta\nu - a_2\Delta\nu e^{-(\Delta\nu/a_3)} \quad (1)$$

the same employed in ref 18, has been used to describe the frequency shift with pressure of the nitrite band. The values of the three fitting parameters a_1, a_2, and a_3 are reported in Table 1 for the different temperatures.

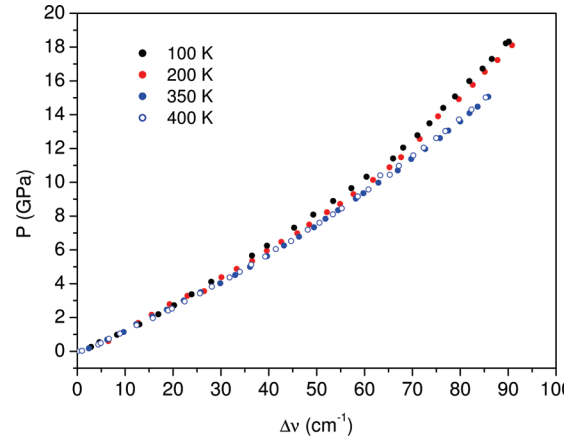

Figure 1. Evolution with pressure at different temperatures of the frequency shift ($\nu(P)-\nu(0)$) of the antisymmetric stretching mode (ν_3) of the NO_2^- ion in NaBr. Equation 1 has been used to reproduce the experimental data, the fitting parameters are reported in Table 1.

TABLE 1: Fitting Parameters of the Nitrite Antisymmetric Stretching Mode Pressure Shift ($\Delta\nu$) According to Eq 1 at All the Different Experimental Temperatures

T (K)	a_1 (GPa/cm^{-1})	a_2 (GPa/cm^{-1})	a_3 (cm^{-1})
100	0.425	0.319	255
200	0.421	0.320	255
300	0.376	0.277	255
350	0.332	0.226	255
400	0.341	0.231	255

We carefully checked the inertness of the salt with respect to the reactive process. The integrated absorption of the nitrite peak used for the pressure measurements remains constant during all the kinetic studies, thus excluding its active participation in the chemical reaction. In addition, to check any catalytic effect of the salt we performed a room temperature experiment with a pure CO sample. The threshold pressure of the reaction, the time scale of the process, and the reaction products were exactly the same in the CO plus salt and pure CO experiments. In the pure CO sample the pressure was determined by the frequency of the first overtone of the CO stretching mode at 4150 cm^{-1} using the frequency of this band in a CO plus salt experiment as a calibration.

3. Results

We have studied the purely pressure induced reaction by FTIR spectroscopy at four different temperatures: 100, 200, 300, and

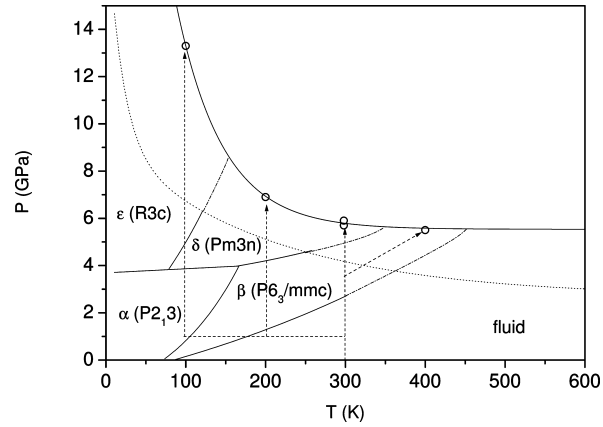

Figure 2. Phase diagram of CO after the present study. The empty circles indicate the $P-T$ values where the onset of the chemical reaction was observed completely avoiding visible or higher frequency irradiation of the sample. The curve fitting of these data is the instability line resulting from this work, and it is compared with that from ref 15 (dotted line) where the sample was somehow always irradiated. The dashed lines indicate the paths followed to reach the experimental conditions where the chemical reaction was observed to occur. Dash−dot lines represent the extrapolated high $P-T$ boundaries of the melting line and of the $\beta-\delta$ and $\delta-\epsilon$ phase boundaries with respect to existing literature data (full lines).

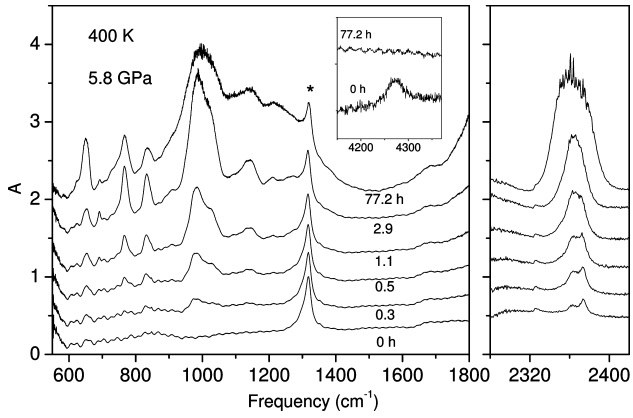

Figure 3. Time evolution of the IR spectra during the chemical transformation occurring at 400 K and 5.8 GPa. In the left panel the band marked by the asterisk is the antisymmetric stretching mode of NO_2^- employed for the pressure measurement. In the inset the overtone of CO at the beginning and at the end of the reaction is reported. In the right panel the band corresponding to the antisymmetric stretching mode of CO_2 is shown.

400 K. In the low temperature experiments the samples were first isobarically cooled at ∼1 GPa to the temperature of the experiment and then slowly compressed at constant temperature. The same procedure could not be adopted for the measurement at 400 K because at this temperature the characteristic spectroscopic signatures of the reaction (see below) were observed immediately when the fluid CO was compressed above 1 GPa. As shown in Figure 2, the study of the reaction at this temperature was possible only by keeping the sample in the β crystal phase and achieving the reaction conditions through a simultaneous compression and heating of the sample. The onset of the chemical reaction was identified by the appearance of several new bands. The best indicator of the reaction onset is a band around 1000 cm^{-1} which is the most intense absorption in all the experiments (see Figure 3). The $P-T$ conditions where the reaction threshold was observed in this work are reported in Figure 2. These data are the results of different experiments using different freshly loaded samples completely avoiding any

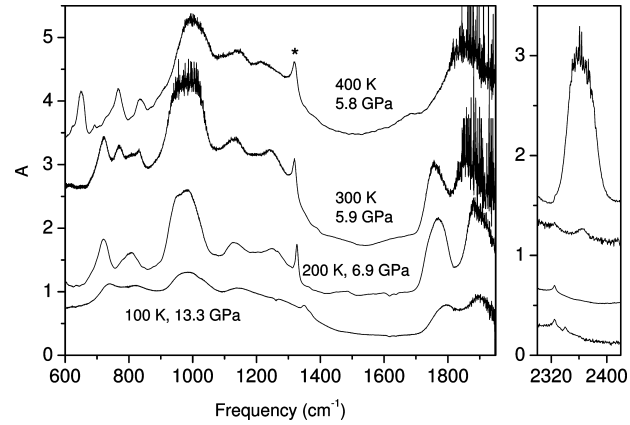

Figure 4. IR spectra measured after the achievement of the equilibrium at the different pressures and temperatures where the reaction was studied. The band marked by the asterisk is due to the antisymmetric stretching mode of NO_2^- employed for the pressure measurement.

visible or higher energy irradiation of the sample. From Figure 2 it is evident that the instability line measured in this work lies well above that reported in ref 15, especially at low temperature. Another remarkable feature of the present experiment is that we have induced the reaction from three different crystal phases, namely, the fully ordered rhombohedral ϵ (100 K), the partially ordered cubic δ (200 and 300 K), and the disordered hexagonal β (400 K).

3.1. Spectra. In all the experiments we have monitored the time evolution of the CO reaction at constant P (±0.1 GPa) and T (±0.1 K) by FTIR spectroscopy, as reported in Figure 3 for the 400 K experiment. The time required for the reaction to reach the completion ranges from less than 10 h at 400 K to about 200 h at 100 K. Only at 400 K is the CO 100% transformed, whereas at all the other temperatures the amount of transformed CO is 70 ± 1%. This estimation was performed by monitoring the integrated absorbance of the CO stretching overtone band at ∼4270 cm^{-1} at the beginning and at the end of the reaction (see inset of Figure 3). Some differences can be observed among the product spectra obtained in the different isothermal compression experiments. In Figure 4 we compare the last spectrum measured at the end of the kinetic study for each temperature. Despite the different broadening of the absorption patterns due to the different P and T conditions, we can easily compare the spectra measured in the various experiments. The region between 900 and 1300 cm^{-1} is quite similar in all the four products, showing three maxima at about 990, 1130, and 1240 cm^{-1}. These absorptions are related to the stretching modes of C−C−O and C−O−C groups[20] and roughly indicate that the bulk of the product is very similar in all the experiments. The broadness of these peaks and the lack of significant changes with pressure support the absence of long-range order of this network, as suggested either by ab initio calculations[17] or by the experimental studies of refs 14 and 15. On the contrary, the spectra are rather different below 900 cm^{-1} as well as in the carbonyl (1755 cm^{-1}) and CO_2 (2360 cm^{-1}) asymmetric stretching regions. As a matter of fact, the formation of CO_2 is not observed in the low temperature measurements; only traces of it are present at 300 K, whereas a huge amount, roughly 30 times larger than at 300 K, forms at 400 K. The formation of CO_2 is accompanied by a clear change in the carbonyl stretching absorption region, where the band at ∼1755 cm^{-1} becomes barely visible, thus suggesting a competition between the formation of the two species. However, the greatest source of information about the reaction is the spectral region

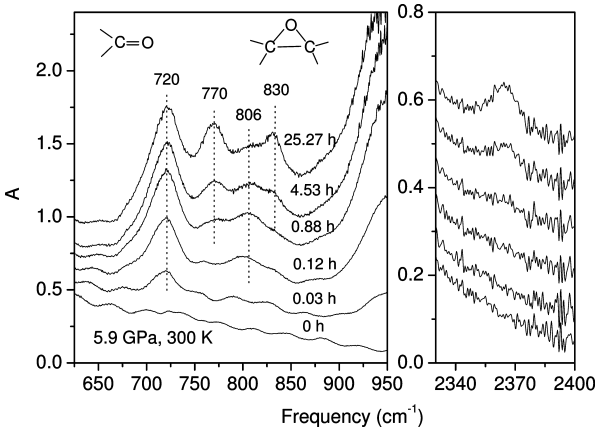

Figure 5. Time evolution of the IR spectra measured in the low frequency (left panel) and CO_2 stretching (right panel) regions in a room temperature experiment. Carbonyl (responsible of the bands at 720 and 806 cm^{-1}) and epoxy ring (responsible of the bands at 770 and 830 cm^{-1}) groups are also reported in the left panel.

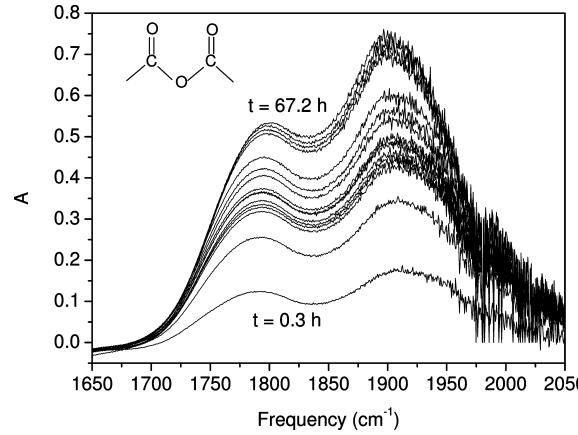

Figure 6. IR spectra of the C═O stretching region measured during the reaction at 100 K and 13.3 GPa. These spectra have been obtained by subtracting the spectrum measured at the beginning of the kinetic study ($t = 0$) to increase the signal-to-noise ratio. The two peaks are assigned to the symmetric and antisymmetric C═O stretching modes of anhydride groups (see inset).

below 900 cm^{-1}. Here, besides the CO_2 bending mode at 650 cm^{-1}, visible only in the 400 K experiment, four bands can be identified at 720, 770, 806, and 830 cm^{-1} (frequency values at room temperature). These four peaks are simultaneously observed only in the room temperature reaction, whereas only the peaks at 720 and 806 cm^{-1} are observed in the low temperature experiments and those at 770 and 830 cm^{-1} in the 400 K reaction. The time evolution of the ambient temperature reaction, reported in Figure 5, provides an insight on the dynamics of the transformation process. The two bands observed in the low temperature experiments, at 720 and 806 cm^{-1}, are the first to be detected and rapidly intensify up to the appearance of the other two bands at 770 and 830 cm^{-1} and of the CO_2 antisymmetric stretching band at 2360 cm^{-1}. The two bands at 770 and 830 cm^{-1} are extremely characteristic of three-membered cyclic ethers (epoxy rings) and correspond respectively to the symmetric and antisymmetric ring deformation, whereas the peaks at 720 and 806 cm^{-1} can be assigned to the bending mode of carbonyl groups.[20] This assignment is consistent with the results of the 400 K experiment where this latter doublet is not observable and also the presence of the most intense C═O stretching band at ~1755 cm^{-1} is questionable. A careful analysis of the C═O stretching region provides valuable information about the product composition. The low temperature experiments clearly show in this region two strong absorptions peaked at 1770−1780 and 1900−1920 cm^{-1}, the latter being slightly stronger (see Figure 6). The high frequency band is not observable in the ambient temperature spectrum because the increasing broadening with rising temperature of the diamond band makes its observation difficult. The high frequency of the carbonyl stretching mode and the presence of a doublet point unambiguously to the formation of an anhydride.[20] Nevertheless, much weaker absorptions are revealed by the bands deconvolution in the low frequency side of this doublet, suggesting the presence of carbonyl groups of a different kind.

3.2. Kinetics. To obtain the kinetic information, we have studied the time evolution of the integrated absorbance of the products and reactant bands that could be unambiguously assigned. Specifically, the absorption bands relative to the CO_2 and carbonyl stretching and bending modes, to the symmetric and antisymmetric deformation of the epoxy ring and to the first overtone of CO, were reproduced by pseudo-Voight profiles, thus obtaining the corresponding integrated absorbances. In this analysis we did not consider the broad bands between 900 and 1300 cm^{-1} because of the difficult identification of the specific absorptions and of the strong intensity of the most intense band at 990 cm^{-1} that is often out of scale, thus precluding a reliable intensity analysis. In the 400 K experiment the asymmetric stretching mode of CO_2 reached the saturation. In this case the integrated area of the bending mode (~650 cm^{-1}), measured in the early stages of the reaction together with that of the asymmetric stretching mode (~2360 cm^{-1}), was employed to calculate the stretching absorption. The plots of the kinetic data relative to the CO overtone, to the carbonyl, and to the epoxy groups measured in the room temperature experiments are reported in Figure 7. To interpret these data, we used the Avrami law[21] originally developed for the crystal growth from a liquid phase but successfully employed in reproducing the growth of extended materials such as polymers and oligomers.[2,3,18,22−25] Two analytical functions have been employed to reproduce respectively the CO decrease

$$B(t) = B_0 - (B_0 - B_\infty)(1 - \exp^{-[k(t - t_0)]^n}) \quad (2)$$

and the products growth

$$A(t) = A_\infty(1 - \exp^{-[k(t - t_0)]^n}) \quad (3)$$

A and B are respectively the product and the reactant concentrations (in our case their integrated absorbance) with the subscripts 0 and ∞ indicating the beginning and the completion of the reaction, respectively. k is the rate constant, n a parameter accounting for the dimensionality of the growth process, and t_0 the beginning of the reaction on the time scale of the experiment. The same k and n parameters have been successfully employed in the fit of the kinetic evolution of different bands relative to the same species, thus confirming their assignment. In Table 2 these parameters are reported for all the kinetic studies.

A different approach should be used to treat the CO_2 formation. The two simplest sources of CO_2 are the decomposition of the extended amorphous network, as suggested in ref 15, and the direct reaction of two CO molecules. In principle the two reactions could be identified from the kinetic data because a first- and a second-order kinetics, respectively, should be expected for the two types of reaction. In Figure 8 we report the time evolution of the integrated area of the antisymmetric stretching mode of CO_2 at 300 and 400 K and the linear plot

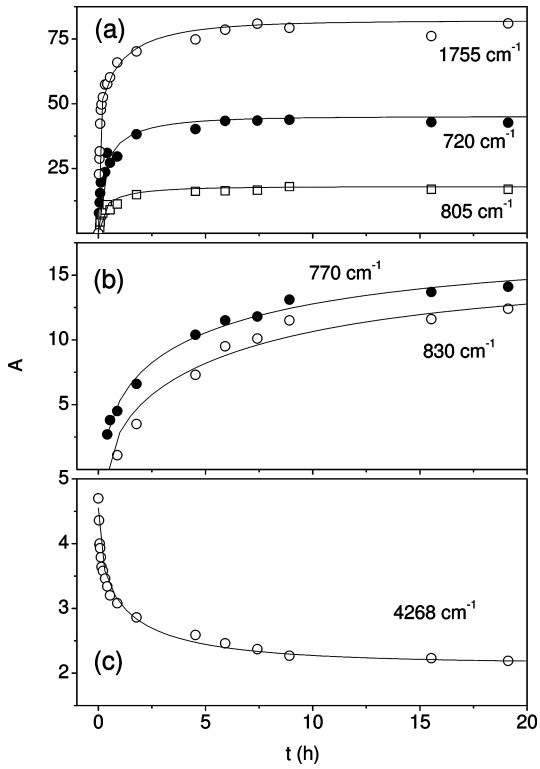

Figure 7. Room temperature kinetic study of the carbonyl stretching (1755 cm^{-1}) and bending modes (a), of the epoxy ring deformations (b) and of the CO overtone (c). Equation 3 has been employed to reproduce the data in (a) and (b), whereas for the CO overtone data we have used eq 2. Only the low frequency band of the C═O stretching mode was fitted due to the overlapping of the diamond absorption band with the higher frequency C═O stretching peak. The fitting data are reported in Table 2.

TABLE 2: Fitting Parameters of the Kinetic Curves According to the Avrami Model[a]

	frequency (cm^{-1})	k (h^{-1})	n	t_0 (h)
	13.3 GPa, 100 K			
overtone CO	4274	0.26	0.4	0
carbonyl str.	1910	0.08	0.4	0
carbonyl str.	1787	0.08	0.4	0
carbonyl bend.	817	0.08	0.4	0
carbonyl bend.	737	0.09	0.4	0
	6.9 GPa, 200 K			
overtone CO	4268	0.23	0.5	0
carbonyl str.	~1900			0
carbonyl str.	1766	0.38	0.5	0
carbonyl bend.	810	0.38	0.5	0
carbonyl bend.	720	0.38	0.5	0
	5.9 GPa, 300 K			
overtone CO	4268	0.85	0.5	0
carbonyl str.	1756	2.10	0.5	0
carbonyl bend.	805	2.22	0.5	0
carbonyl bend.	720	2.21	0.5	0
epoxy	830	0.4	0.18	0.5
epoxy	770	0.4	0.20	0.3
	5.8 GPa, 400 K			
overtone CO	4268	1.15	0.5	0
epoxy	830	0.55	1	0.3
epoxy	770	0.53	1	0.5

[a] The data relative to the first overtone of CO have been obtained by using eq 2, and eq 3 was employed for all the other bands. Reliable data for the kinetic analysis of the high frequency carbonyl stretching band have been obtained only in the 100 K experiment.

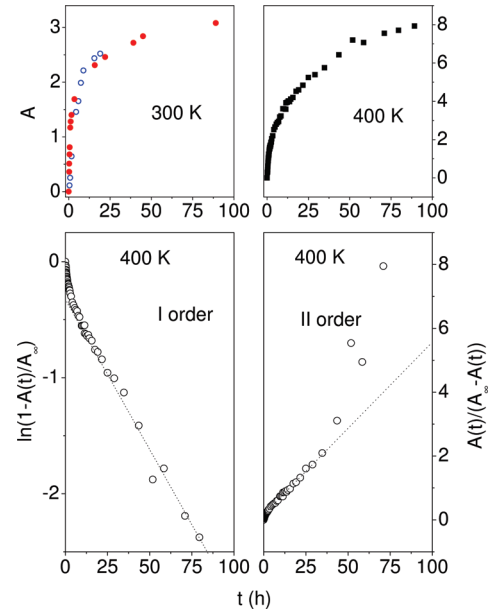

Figure 8. Kinetic data relative to the CO_2 formation in the 300 and 400 K experiments (upper panels). Two different sets of data are reported for the room temperature experiment. In the lower panels the linear plot for a first- (left) and a second-order (right) reaction are reported for the 400 K data. Dotted lines are eye guides to show the linear behavior at long (first-order, left panel) and short (second-order, right panel) reaction times.

for first- and second-order kinetics at 400 K. As can be seen, neither of the two laws allows the 400 K experimental data to be reproduced in the full time interval, suggesting that a more complex rate law characterizes the CO_2 formation. However, linearity regions can be identified on different time scales for both first- and second-order kinetics. A second-order kinetics satisfactorily reproduces the data in the early stages of the reaction ($t \leq 17$ h), excluding the very beginning where nucleation effects can alter the kinetic profile, whereas a first-order mechanism can be used in the long time regime. This result may indicate the existence of different channels for the CO_2 formation. The kinetic data reported in the upper panels show that in both cases, 300 and 400 K, the equilibrium amount of CO_2 is not reached even after ~100 h. This behavior is similar to that of the epoxy species (see Figure 7) but differs from the evolution with time of the carbonyl group concentration.

3.3. Recovered Samples. The spectra of the reaction products are not substantially altered once the ambient conditions are recovered. The only detectable change is a small amount of carbon dioxide that forms in the samples produced in the low temperature experiments (see Figure 9). On the contrary, all the samples are dramatically altered once the cell is opened and the products exposed to the atmosphere. The comparison between the spectra measured just before and after the opening of the cell is shown in Figure 10 for the product synthesized in the lowest temperature experiment (100 K), but all the samples look the same after the cell opening, independent of the temperature of the experiment. The three panels of Figure 10 show the significant portions of the spectra where the changes are detected. In the low frequency region, left panel, there are remarkable changes concerning the carbonyl absorptions both in the bending and in the stretching regions. In particular, the doublet relative to the C═O stretching mode is substituted by a single band at about 1760 cm^{-1}, whereas in the bending region a broad unstructured band at 750 cm^{-1} replaces the structured spectrum recorded before opening. In addition, a clear intensity

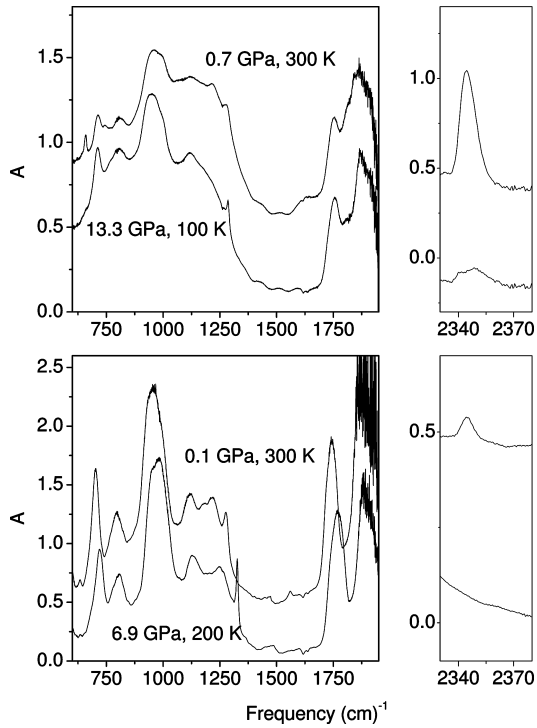

Figure 9. Comparison between the spectra measured at 100 K (upper panels) and 200 K (lower panels) at the end of the reaction and in the closed cell at ambient temperature after the complete release of the pressure in the DAC membrane. These conditions were obtained by first releasing the membrane pressure at the experiment temperature and then by warming up to 300 K.

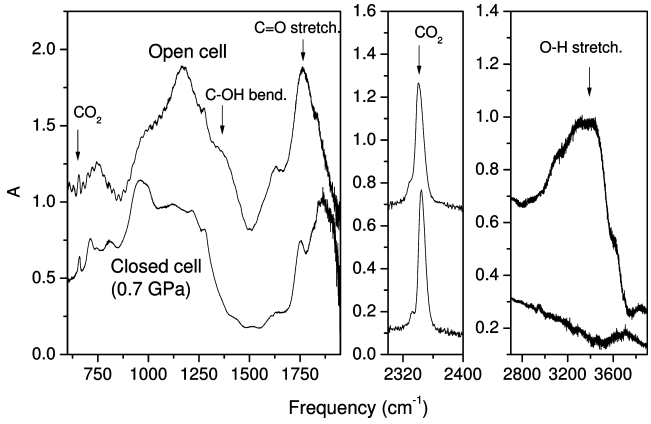

Figure 10. Comparison between the recovered product from the 100 K reaction before and after the opening of the cell in the laboratory atmosphere.

transfer occurs in the 900−1300 cm^{-1} frequency region from the band measured around 990 cm^{-1}, common to all the products at the end of the reaction (see Figure 4), to the band at ∼1170 cm^{-1}. The spectral changes consequent to the cell opening are completed by the appearance of new peaks that are easily assigned to motions involving the hydroxyl group (−OH): a strong and broad band centered at ∼3370 cm^{-1} (O−H stretching mode) and a prominent shoulder at 1375 cm^{-1} assigned to the C−OH bending mode. A shoulder on the low frequency side of the O−H stretching band could possibly indicate also the presence of C−H stretching modes of unsaturated carbon atoms. Finally, the last comment concerns with the presence of CO_2 after the cell opening. This could be ascribed to the trapping of this gas molecules by the extended amorphous network.

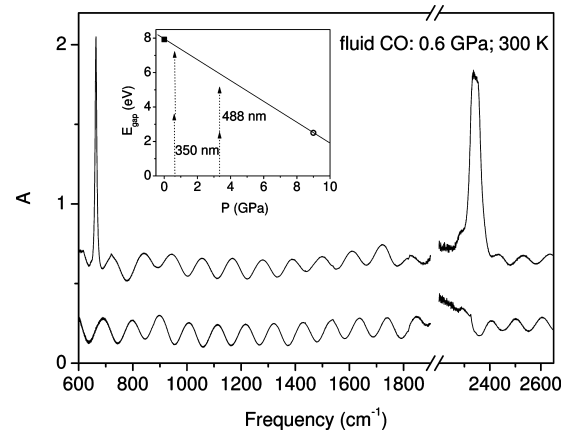

Figure 11. Comparison between the IR spectra of fluid CO measured at 0.6 GPa immediately before (lower trace) and after 3 h of irradiation with 100 mW of the 350 nm Ar^+ laser multiline emission (upper trace). The CO_2 formation is revealed by the appearance of both bending (665 cm^{-1}) and antisymmetric stretching (2345 cm^{-1}) modes. The oscillation of the baseline is due to the interference fringes between the two diamond surfaces delimiting the sample region (∼40 μm). In the inset the $S_0 \rightarrow S_1$ transition energy (E_{gap}), measured at ambient pressure (full square)[26] and computed at 9 GPa (empty circle),[17] are compared with the two-photon energies of this experiment (350 nm) and that reported in ref 15 (488 nm). The full line is a linear eye guide to follow the pressure evolution of the E_{gap}.

4. Discussion

The characterization of the purely pressure induced reactivity of carbon monoxide was performed along four different isotherms in the 100−400 K temperature range, taking advantage of the FTIR technique to monitor the reaction evolution and of infrared sensors for pressure calibration. The careful determination of the onset of the chemical reaction has allowed the purely pressure induced instability boundary to be precisely drawn. This boundary appears significantly shifted to higher pressure with respect to that reported in ref 15 which was determined by IR and Raman measurements and where irradiation of the sample with laser light was somehow always involved in the experiment. The upward shift is particularly evident at low temperature where the difference in the threshold pressure is as large as 6.5 GPa at 100 K. The effect of laser light in activating the chemical reaction has already been reported, and the photoactivated instability boundary was set to 3.2 GPa at 300 K.[15] However, this information is only qualitative because the photoinduced threshold pressure for the reaction strongly depends on the irradiation wavelength. As a matter of fact, we have been able to trigger the chemical reaction also in the fluid CO at 0.6 GPa and room temperature by using near UV light at 350 nm (see Figure 11). A heterogeneous product formed by CO_2 and a brownish solid, whose very small amount did not allow its characterization, was obtained. Also in ref 15 a large amount of CO_2 was reported to form after the irradiation at 3.2 GPa with visible (488 and 514 nm) light. The mechanism of the photoinduced reaction likely involves the two-photon excitation of the lowest electronic excited $A^1\Pi$ singlet state (S_1). This transition is indeed two-photon allowed and its origin has been measured at 63 880 cm^{-1} (∼7.9 eV) in solid CO at 10 K and ambient pressure.[26] No experimental data exist on the high pressure evolution of these states, but a red shift of the electronic gap from the ambient pressure value to 2.5 eV at 9 GPa was calculated by Bernard et al.[17] This red shift appears extremely large, but assuming its linear evolution with pressure, it is in qualitative agreement with a two-photon absorption process

induced by the wavelength employed here (350 nm at 0.6 GPa) and in ref 15 (488 and 514 nm at 3.2 GPa), as shown in the inset of Figure 11. This behavior could also explain the marked difference characterizing the reactivity of CO and N_2 molecules that cannot be explained in terms of the small dipole moment possessed by CO at ambient conditions. The remarkable pressure shift of the electronic excited states of CO implies the occurrence of a consistent modification of the electronic structure with pressure. The mixing of the ground with the lowest electronic excited states, characterized by a considerable increase of the dipole moment,[27] can lead to the formation of highly reactive species, like those recently reported for benzene,[28] that trigger the high pressure instability.

An important aspect of this study is related to the activation of the reaction from three different crystal phases: the likely rhombohedral ϵ (100 K), the cubic δ (200 and 300 K), and hexagonal β (400 K) phases. Despite the different crystal structures, all the reactions give rise to a solid product showing very similar characteristics, the main difference being the CO_2 formation. More precisely, the same material is obtained in the low temperature experiments, 100 (ϵ) and 200 K (δ), independently of the crystal phase. Small differences are observed in the two reactions studied at 200 and 300 K within the same δ phase. The epoxy rings and the CO_2 formation revealed at 300 K are indeed not observed at 200 K, whereas they are clearly revealed at 400 K where the reaction occurs from the β phase. Also, the results of the kinetic analysis do not evidence any peculiarity relative to the crystal structure. The Avrami kinetic law could be always used to picture the growth mechanism of the extended solid. The value of 0.5 for the n fit parameter found for all the reactions up to room temperature indicates a linear growth of the extended solid preceded by a diffusion step, which is actually the rate determining step of the whole process. At 400 K the n value doubles with respect to all the lower temperature experiments, thus indicating a dimensionality increase of the extended solid formation. The rate constants increase with temperature of an order of magnitude in spite of the very different pressure conditions, 13.3 GPa at 100 K with respect to 5.8 GPa at 400 K. All these data suggest that the reactivity of CO is mainly governed by the temperature rather than the crystal structure. The effect of the temperature, which determines the amplitude of translational and librational lattice motions, joined to the head-to-tail disorder characterizing all the CO crystalline structures, can be responsible for the production of the same material irrespective of the starting crystal. The dominant role of the lattice modes in triggering the chemical reactions in crystals under pressure has been evidenced in several systems[18,22,24] and quantified in the benzene case.[29]

The spectra measured during the reaction at 300 K indicate the existence of two reaction channels (see Figures 5 and 7). In the early stages the reaction behaves as the low temperature experiments with the formation of carbonyl groups. Nevertheless, after about half an hour also the absorption bands of CO_2 and of the epoxy rings are detected while, simultaneously, the growth of the carbonyl bands slows down. At 400 K only the second channel seems to be active, as indicated by the huge amount of CO_2 formed and by the detection of the only epoxy rings bands in the bending region. It is not simple to establish whether these two reactive paths are competing or represent two sequential steps of the same reaction mechanism. In the latter case the extended network, containing several carbonyl bonds, would decompose through a decarboxylation process, giving rise to a carbon enrichment of the solid product where the epoxy rings are clearly identified. There are some hints indicating the two-step process as the most probable. First, the formation of CO_2 is also observed when the ambient conditions are recovered after the low temperature reactions (see Figure 9), a process likely due to the decomposition of the low temperature product. Second, the kinetic curves (see Figures 7 and 8) clearly show that at room temperature a constant concentration of the carbonyl species is reached after 4−5 h, while both the epoxy rings and CO_2 bands are still growing up even at the end of the experiment. However, a conclusive confirmation of the two-step mechanism could be provided, within this approach, only by the observation of an intensity decrease of the carbonyl bands that is not the case on the time scale in which we have studied the reaction. Finally, at 300 K the epoxy rings and the CO_2 formation are appreciably delayed with respect to the carbonyl formation. Such a temporal separation could indicate a consecutive rather than a parallel reactive process. A similar two-step mechanism was also proposed in ref 15 where the initially formed polymer was indicated to disproportion to a solid product and CO_2, and in ref 17 where some of the carbonyl groups of the linear chains formed in the first step were reported to open, giving rise to 5-fold cycles. Some more insight on the reaction mechanism could be obtained from the formation kinetics of CO_2 that we have tried to reproduce by simple first- and second-order rate laws. As a matter of fact, a first-order kinetics could support the decarboxylation of the solid product and thus the two-step mechanism. Nevertheless, the kinetic data are better reproduced by a second-order kinetic law in the early stages of the reaction, whereas a first-order kinetics nicely agrees after 17 h from the beginning, thus suggesting a more complex reaction mechanism. This result can be tentatively interpreted as due to the initial CO_2 formation from the direct reaction of two CO molecules. Then, as the reaction proceeds, the first-order mechanism could suggest the decomposition of the extended network to become the primary CO_2 source.

In this work we have made a big effort to provide a precise characterization of the reaction product. Figure 10 clearly illustrates how the characteristics of the material produced in the reaction dramatically change when the cell is opened. As a consequence, all the literature data obtained on samples after the cell opening (see ref 15), regardless of the employed technique, are related to another product resulting from the reaction between the high pressure synthesized material and the atmosphere. In our study, the spectra of the solid material formed during the reaction do not present any band ascribable to atoms different from C and O and appear rather different from those reported in literature[13−15] that, on the other hand, are very similar to the spectra we have measured after the cell opening. As already stated in the presentation of the spectra, the doublet observed in the carbonyl stretching region and the high frequency values of these peaks unambiguously point to the identification of anhydride groups. The two peaks correspond to the in- and out-of-phase vibrations of the two carbonyl groups that at ambient pressure are generally observed between 1715 and 1870 cm^{-1}.[20] In cyclic anhydrides the lower frequency band is 11 to 3 times stronger than the high frequency one depending on the anhydride type. On the contrary, in unconjugated noncyclic anhydrides this intensity ratio is inverted, with the high frequency band 1.05−1.25 times stronger. The latter case nicely adapts to our observation (see Figure 6), being also supported by the kinetic data that account for a linear growth of the reaction product. The formation of noncyclic anhydrides is also supported by the analysis of the C−C−O and C−O−C

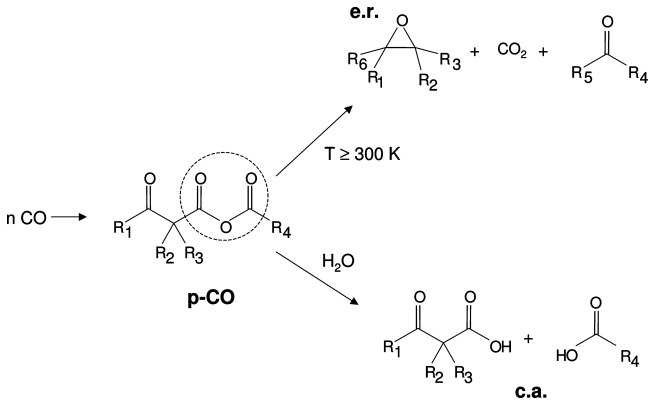

Figure 12. Proposed scheme for the pressure induced reaction of carbon monoxide. The polycarbonyl (p-CO) chains formed by the reaction of the CO molecules contain a considerable amount of anhydride groups (evidenced by the dotted circle). This product likely decompose at $T \geq 300$ K giving rise to epoxy rings (e.r.) and carbon dioxide, and readily reacts with atmospheric water to give the corresponding carboxylic acid (c.a.). R_i indicate substituent chains or fragments attached to the groups of interest.

stretching region. The absorption bands relative to these modes are expected in the 1000−1150 and 880−950 cm^{-1} frequency regions for noncyclic and cyclic anhydrides, respectively. In our spectra a very strong band is indeed observed just below 1000 cm^{-1}. It should be remarked that our IR spectra are completely different from that of poly(carbonyl suboxide),[30] allowing us to rule out the formation of this material whose formation was suggested by several authors.[11,14,15]

After the cell opening the product reacts with the atmospheric water, as clearly indicated by the new bands involving the OH group (at 3370 and 1375 cm^{-1}) (see Figure 10). In addition, other spectral changes, such as the intensity redistribution in the 900−1300 cm^{-1} spectral region, point to the conversion of the anhydride groups into different chemical species. Hydrolysis of anhydrides leads to the formation of carboxylic acids. Several regions of the IR spectrum are useful to identify the carboxylic acids bands. A strong absorption is expected near 3000 cm^{-1} due to the OH stretching mode with a variable frequency and bandwidth depending on the degree of association. The C═O stretching falls around 1760 cm^{-1}, shifting to lower frequencies (∼1650 cm^{-1}) in dimeric forms. Both bands are found in the spectra measured after the opening of the cell and the frequency of the carbonyl stretching and the relative narrowness of the O−H stretching mode suggest a nondimeric acid. This conclusion is also supported by the broad band observed at 750 cm^{-1} that is probably due to the out-of-plane wagging of hydrogen bonded OH···O groups. In dimeric carboxylic acid this broad band falls between 960 and 875 cm^{-1} while it shifts to lower frequency when a nondimeric form of hydrogen bonding involves the COOH group. The strong peak at 1190 cm^{-1} due to the C−O stretching, even if less indicative, is in nice agreement with the expected frequency for these modes in carboxylic acids. The C−O−H in plane bending is seen between 1440 and 1395 cm^{-1}.

On the basis of this discussion, we can therefore draw a possible scheme for the pressure induced reaction of carbon monoxide in the investigated $P-T$ range (see Figure 12).

(a) In general, the reaction gives rise to an extended solid made by polycarbonyl chains containing linear anhydrides groups whose formation is probably due to the head-to-tail disorder of the CO crystals. For $T < 300$ K this is the only product and no CO_2 is formed.

(b) At $T \geq 300$ K a new reaction process leading to the formation of epoxy rings and CO_2 is activated. This is also the only process observed at 400 K. There are not conclusive evidence to identify if this is a competitive reaction channel or is the spontaneous decarboxylation of the polycarbonyl chains. Some hints indicate the latter two-step mechanism as the preferred one.

(c) The reaction of the recovered sample with atmospheric water produces nondimeric carboxylic acids groups.

5. Conclusion

This study on the pressure induced reactivity of solid CO reveals the complexity of the chemical processes taking place under high pressure conditions even for the simplest molecular systems. The understanding of the mechanisms regulating the reactivity at high pressure is subordinated to the careful control of the different parameters that determine the reaction path. Pressure, temperature, and photoirradiation all contribute to establish the onset of the chemical reaction as well as the reactive path. Pressure tunes the intermolecular interactions, allowing the exploration of unlikely accessible high energy regions of the fundamental potential energy surface where relevant changes of the molecular electronic distribution take place. Temperature rules the amplitude of the lattice motions thus allowing reactive configurations to be realized. Finally, photoexcitation produces molecules with geometrical and electronic properties completely altered with respect to the fundamental state which can act as reaction initiators. In this work the pressure induced reactivity of CO was studied by successfully uncoupling the effects of the three parameters $P-T-h\nu$ by performing isothermal compression studies at four different temperatures (100−400 K), completely avoiding laser irradiation. This was possible by using $NaNO_2$ sensors to measure the sample pressure and FTIR spectroscopy to monitor the reaction evolution and to characterize the reaction products. Anhydride groups characterize the extended disordered solid, formed by interconnected linear chains, obtained from the low temperature syntheses. The presence of other chemical groups like ethers, esters and ketones, even though not demonstrated, is probable due to the disordered nature of the material. At room temperature a new reaction channel opens giving rise to the formation of CO_2 and epoxy rings. This process is the only detectable at 400 K. Several hints indicate that the formation of these species is due to the decarboxylation of the anhydride groups. The product obtained by all the reactions is unstable and readily reacts with atmospheric water once the cell is opened. Carboxylic groups form by the hydrolysis of anhydrides, but evidence of a more general saturation of the solid product are obtained by the observation of C−H and O−H groups. The difference existing between the photoinduced reactivity of the isostructural CO and N_2 molecules has been rationalized on the basis of a remarkably different pressure shift of the electronic excited states.

Acknowledgment. Supported by the European Union under Contract RII3-CT2003-506350, given by the Italian Ministero dell'Università e della Ricerca Scientifica e Tecnologica (MURST) and by "Firenze Hydrolab" through a grant by Ente Cassa di Risparmio di Firenze.

References and Notes

(1) Schettino, V.; Bini, R.; Ceppatelli, M.; Ciabini, L.; Citroni, M. In *Advances in Chemical Physics*; Rice, S. A., Ed.; Wiley: New York, 2005; Vol. 131, pp 105−242.

(2) Citroni, M.; Ceppatelli, M.; Bini, R.; Schettino, V. *Science* **2002**, *295*, 2058.
(3) Chelazzi, D.; Ceppatelli, M.; Santoro, M.; Bini, R.; Schettino, V. *Nat. Mater.* **2004**, *3*, 470.
(4) McMillan, P. F. *Nat. Mater.* **2002**, *1*, 19.
(5) Hemley, R. J.; Mao, H. K. *Mineral. Mag.* **2002**, *66*, 791.
(6) Iota, V.; Yoo, C. S.; Cynn, H. *Science* **1999**, *283*, 1510.
(7) Santoro, M.; Gorelli, F. A.; Roberto Bini; Ruocco, G.; Scandolo, S.; Crichton, W. *Nature (London)* **2006**, *441*, 857.
(8) Eremets, M. I.; Hemley, R. J.; Mao, H. K.; Gregoryanz, E. A. *Nature (London)* **2001**, *411*, 170.
(9) Eremets, M. I.; Gavriliuk, A. G.; Trojan, I. A.; Dzivenko, D. A.; Boehler, R. *Nat. Mater.* **2004**, *3*, 558.
(10) Katz, A. I.; Schiferl, D.; Mills, R. L. *J. Phys. Chem.* **1984**, *88*, 3176.
(11) Mills, R. L.; Schiferl, D.; Katz, A. I.; Olinger, B. *J. Phys. (Paris), Colloq.* **1984**, *45*, C8–187.
(12) Mills, R. L.; Cromer, D. T. *J. Chem. Phys.* **1986**, *84*, 2837.
(13) Lipp, M. J.; Evans, W. J.; Garcia-Baonza, V.; Lorenzana, H. E. *J. Low Temp. Phys.* **1998**, *111*, 247.
(14) Lipp, M. J.; Evans, W. J.; Baer, B. J.; Yoo, C. S. *Nat. Mater.* **2005**, *4*, 211.
(15) Evans, W. J.; Lipp, M. J.; Yoo, C. S.; Cynn, H.; Herberg, J. L.; Maxwell, R. S. *Chem. Mater.* **2006**, *18*, 2520.
(16) Cromer, D. T.; Schiferl, D.; LeSar, R.; Mills, R. L. *Acta Crystallogr.* **1983**, *C39*, 1146.
(17) Bernard, S.; Chiarotti, G. L.; Scandolo, S.; Tosatti, E. *Phys. Rev. Lett.* **1998**, *81*, 2092.
(18) Ceppatelli, M.; Santoro, M.; Bini, R.; Schettino, V. *J. Chem. Phys.* **2000**, *113*, 5991.
(19) Bini, R.; Ballerini, R.; Pratesi, G.; Jodl, H. J. *Rev. Sci. Instrum.* **1997**, *68*, 3154.
(20) D.Lin-Vien, Colthup, N. B. Fateley, W. G. Grasselli J. G. *The handbook of Infrared and Raman Characteristic frequencies of organic molecules*; Academic Press, Inc.: San Diego, 1991.
(21) Avrami, M. *J. Chem. Phys.* **1939**, *7*, 1103; **1940**, *8*, 212; **1940**, *8*, 177.
(22) Citroni, M.; Ceppatelli, M.; Bini, R.; Schettino, V. *J. Chem. Phys.* **2003**, *118*, 1815.
(23) Chelazzi, D.; Ceppatelli, M.; Santoro, M.; Bini, R.; Schettino, V. *J. Phys. Chem. B* **2005**, *109*, 21658.
(24) Citroni, M.; Ceppatelli, M.; Bini, R.; Schettino, V. *J. Chem. Phys.* **2005**, *123*, 194510.
(25) Citroni, M.; Ceppatelli, M.; Bini, R.; Schettino, V. *J. Phys. Chem. B* **2007**, *111*, 3910–3917.
(26) Lu, H. C.; Chen, H. K.; Cheng, B. M.; Kuo, Y. P.; Ogilvie, J. F. *J. Phys. B: At. Mol. Opt. Phys.* **2005**, *38*, 3693.
(27) Drabbels, M.; Meerts, W. L.; ter Meulen, J. J. *J. Chem. Phys.* **1993**, *99*, 2352.
(28) Citroni, M.; Bini, R.; Foggi, P.; Schettino, V. *Proc. Natl. Acad. Sci. U.S.A.* **2008**, *105*, 7658–7663.
(29) Ciabini, L.; A Gorelli, F.; Santoro, M.; Bini, R.; Schettino, V.; Raugei, S. *Nat. Mater.* **2007**, *6*, 39–43.
(30) Snow, A. W.; Haubenstock, H.; Yang, N. L. *Macromolecules* **1978**, *11*, 77.

JP900586A